Physica B 404 (2009) 315–319

Contents lists available at ScienceDirect

Physica B

journal homepage: www.elsevier.com/locate/physb

Growth and optical properties of ZnO microwells by chemical vapor deposition method

C.H. Zang [a,c], Y.C. Liu [b,*], D.X. Zhao [a,*], Y.S. Zhang [c]

[a] Key Laboratory of Excited State Process, Changchun Institute of Optics, Fine Mechanics and Physics, Chinese Academy of Sciences, Changchun 130033, PR China
[b] Center for Advanced Optoelectronic Functional Materials Research, Northeast Normal University, Changchun 130024, PR China
[c] Department of Mathematics and Physics, Luoyang Institute of Science and Technology, Luoyang 471023, PR China

ARTICLE INFO

Article history:
Received 29 August 2008
Received in revised form
10 October 2008
Accepted 4 November 2008

Keywords:
ZnO microwells
Photoluminescence

ABSTRACT

The well-like ZnO nanostructures were obtained by chemical vapor deposition method. The uniform and dense ZnO slim nano-columns were grown along the circle to form a microwell. The growth mechanisms, such as 1D linear, 2D screw dislocation and step growth are discussed. These observations provide some insight into the growth kinetics in vapor–solid growth process. The fabrication of ZnO microwell morphology provided a direct experimental evidence for explaining the 1D growth mechanism based on the axial screw dislocation. Photoluminescence (PL) microscopy showed the surface-related optical properties. The green light emission enhancement revealed that the ZnO microwells have waveguide properties. The abnormal enhancement of integrated PL intensity of deep-level emission with temperature increase showed abundant surface state existence.

© 2008 Elsevier B.V. All rights reserved.

1. Introduction

Semiconductor nanomaterials are attractive building blocks for their potential applications in nanoscale electronic and optical devices. Among these materials, ZnO is a promising candidate for its wide direct band gap 3.37 eV and large exciton binding energy 60 meV at room temperature. Many ZnO nanostructures with abundant morphologies, such as nanowires (NWs) [1], nanobelts [2], nanocombs [3], nanoflowers [4] and nanofingers [5], have been synthesized for their potential application in nanoscale devices such as UV laser, field-effect transistors [6], field emitter [7], nanosensors [8,9] and nanoresonators [10]. Many methods, such as chemical vapor deposition, thermal evaporation, hydrothermal technique and solution phase [11–14], have been attempted to prepare ZnO nanoscale materials. In our experiment, chemical vapor deposition method is adopted. The well-like ZnO nanostructures are obtained through controlled temperature cooling rate. In general, the morphology is decided by thermodynamic process associated with interface energy and interface pressure. The different growth mechanism determined by different interface structure shows different growth velocity, which belongs to growth kinetics. Therefore, the growth mechanisms corresponding to these morphologies are discussed from the point of view of not only thermodynamics but also kinetics. Sears proposed a mechanism: the driving force for 1D growth originates from an axial screw dislocation and incoming atoms could adsorb onto the entire surface of a NW and then migrate toward the growing tip [15]. But, no one was able to observe the proposed screw dislocation in the final product [16].

In this paper, 1D NWs grow along axial screw dislocation curve to form the microwell morphology. The synthesis of ZnO microwell morphology can provide an experimental evidence for 1D growth mechanism based on axial screw dislocation. Moreover, the obtained 1D NWs are with abundant surface and interface defects. To further clarify such nanostructures, photoluminescence (PL) spectra related to the surface and the interface are investigated. The green light enhancement was observed. The light enhancement properties show a promise of application as light source array [17].

2. Experimental details

The well-like ZnO nanostructures were synthesized via chemical vapor phase deposition method in a horizontal tube furnace. The 4N·Zn powder was a source material loaded in a quartz boat. The Si substrates were laid above the source about 3–5 mm. The rapid increase of temperature to 580 °C was kept for 2 h under a ultra-pure N_2 ambient with a flow rate 150–200 SCCM. Then, the power to the furnace was turned off to obtain a fast cooling rate. As the temperature cooled to room temperature, a layer of gray deposition was found on the Si substrates.

Morphology and composition of products were observed by field-emission scanning electron microscopy (SEM, Hitachi

* Corresponding authors. Tel.: +86 431 85099168; fax: +86 431 85684009.
E-mail address: ycliu@nenu.edu.cn (Y.C. Liu).

0921-4526/$ - see front matter © 2008 Elsevier B.V. All rights reserved.
doi:10.1016/j.physb.2008.11.007

S-4800), energy-dispersive X-ray spectroscopy (EDX, GENE SIS 2000 XMS 60S, EDAX, Inc.) attached to the SEM. The structural characterization was analyzed by X-ray diffraction (XRD, Rigaku D/max-rA) spectroscopy with the Cu Kα line of 0.154 nm. The micro-PL spectrometer excited with a He–Cd laser at 325 nm.

3. Results and discussion

3.1. Morphology and structure

A low-magnification SEM image shows the microwells, depicted in Fig. 1(a). The width of microwells ranges from 800 nm to 1.5 μm. The high-magnification SEM images show twins and single microwells in Fig. 1(b,c). Microwells are composed of two parts: under part of the microwell is the microtower and the upper part is the hexagon cross-section with a circular hole at the center, see Fig. 1(c). The width of microtower is about 1.5 μm and the height is about 2 μm. The side of the microtower has light and dark alternative growth layers seen in Fig. 1(d). It might be attributed to mass transport or thermal transport fluctuation caused by the carrier gas, a small periodical fluctuation. The top view of the microwell is a hexagonal cross-section filled with many uniform ZnO nano-columns around the circular hole, depicted in Fig. 2(a). The diameter of the column is

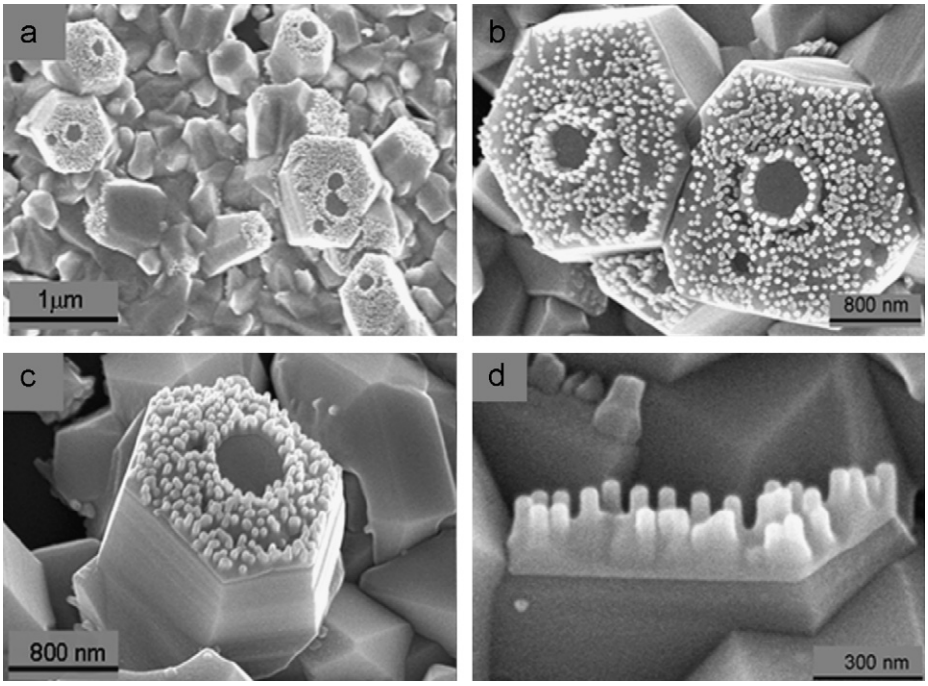

Fig. 1. SEM images of ZnO microwells (a–d).

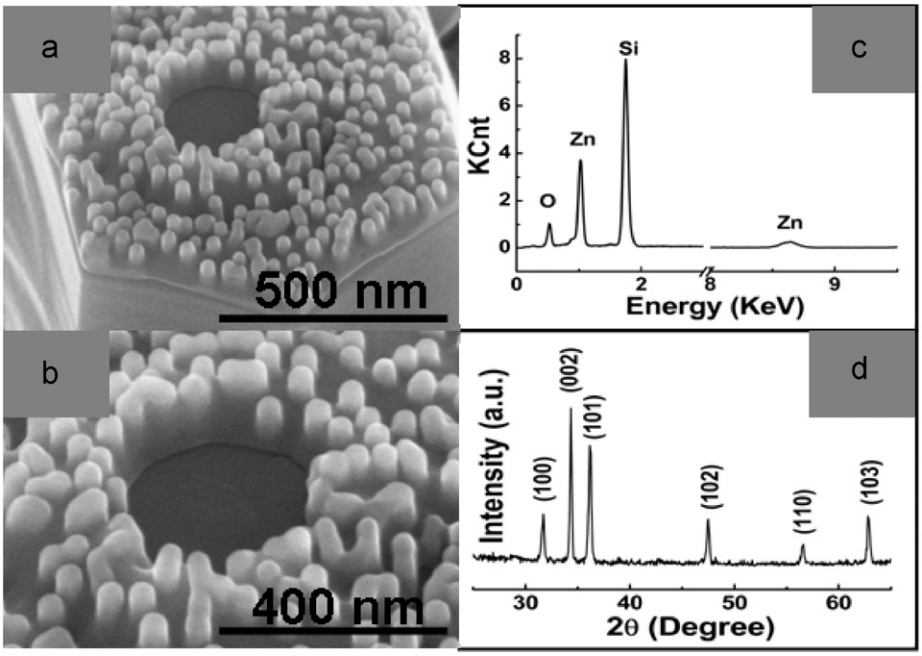

Fig. 2. SEM images of hexagonal cross-section of the ZnO microwells (a,b), EDX spectrum of the ZnO microwells (c) and XRD pattern of the ZnO microwells (d).

about 30–40 nm and the length is about 100 nm, shown in Fig. 2(b).

The EDS indicates that there are only Zn and O elements on the ZnO nanostructures with non-stoichiometric content (Zn:O = 0.52:0.48) shown in Fig. 2(c). It is attributed to growth in N_2 ambient. The ZnO well-like nanostructures show a hexagon wurtzite structure in XRD pattern shown in Fig. 2(d). All peaks can be identified to be diffractive peaks of hexagonal wurtzite ZnO by standard XRD pattern. No other mineral diffractive peak appears, which illustrates that only the ZnO microwells with wurtzite structure formed.

The slim ZnO nano-columns growth process is a homoepitaxy growth process. The influence of seeds on nucleation is explained as follows.

3.2. Seeds

Vayssieres [18] have reported that the seeds have a weak effect on the morphology of ZnO nanostructures. However, morphology and size of ZnO nanostructures are dependent on whether substrates are coated with seeds or not. In our experiment, the ZnO nano-columns grew on the hexagonal cross section, which was as the seeds layer. The NWs are uniform and dense; in the diameter of them is about 30–40 nm. While the ZnO grew on bare Si substrates, the width of the nanotowers is about 1.5 μm. The growth process of the microtower is a heteroepitaxy growth process. There is a higher interface energy between the ZnO crystal nuclei and the Si substrate, compared to that of homo-epitaxy growth. Correspondingly, formation energy of hetero-nucleation is higher than that of homo-nucleation. Probability of crystal nucleation is inversely proportional to the formation energy, which means that the number of nucleus is reduced in the same area, so the width of microtower is observed up to a micrometer. Zhao et al. [19] have reported that it is difficult to grow ZnO NWs on bare Si substrates. In addition, the ZnO seeds layer can increase the surface roughness. The rough surface can absorb and receive atoms, particles and nuclei and further promote the growth of ZnO nanostructures [20]. The growth of small ZnO columns on the microtower is a homoepitaxy growth process. The small column-ZnO arrays are uniform and dense. Dalal et al. [21] have reported that the density of NWs array is determined by the thickness of ZnO seed layer. However, our experimental results show a similar density ZnO nano-columns array on the different height of tower. The density of nano-columns is dependent on the size of nucleus, which is related to formation energy.

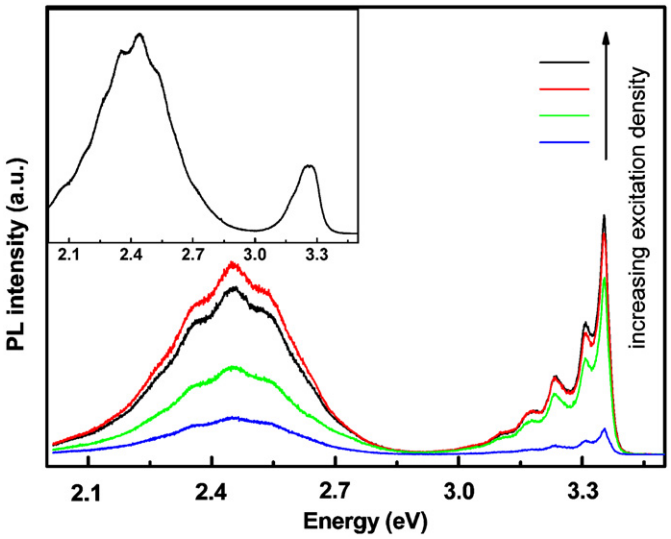

Fig. 4. PL spectra of ZnO microwells at 81 K with a different excitation power density. Inset: room temperature PL spectrum.

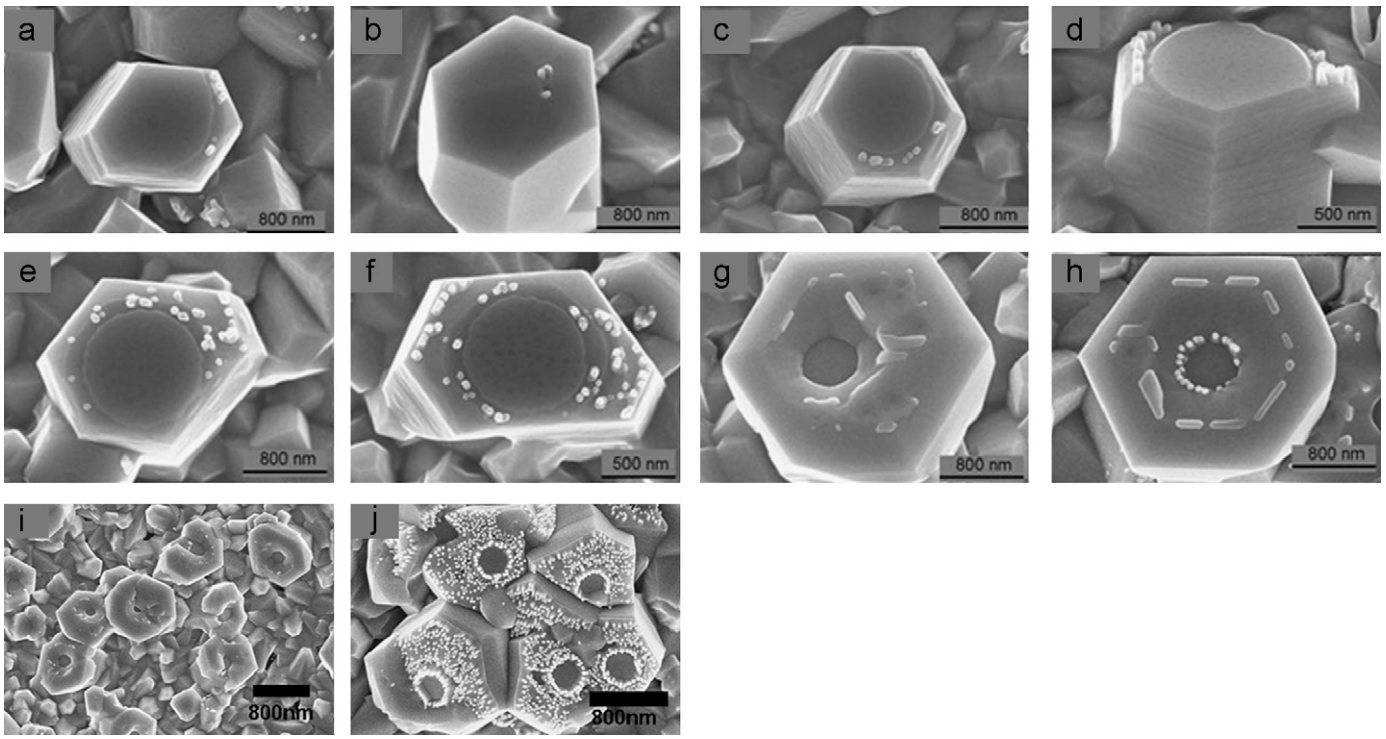

Fig. 3. SEM images of ZnO microwells in the downstream area on the substrate.

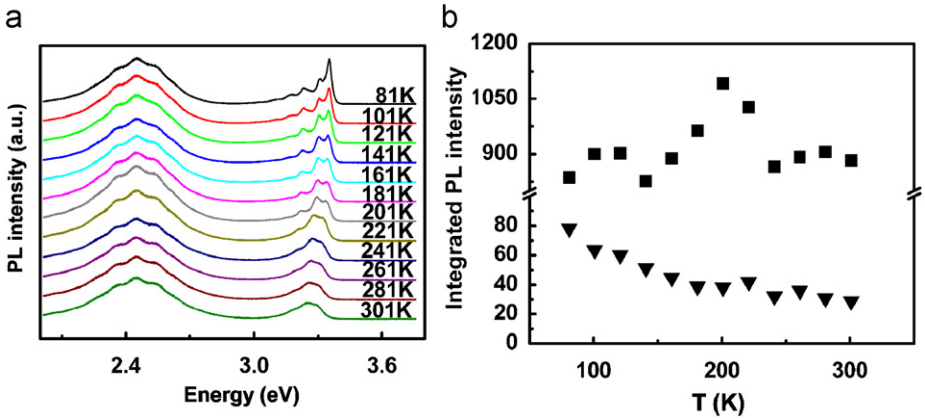

Fig. 5. (a) The temperature dependence PL spectra range 81 –301 K of ZnO microwells and (b) Integrated PL intensity of UV NBE emission (▼) and deep level emission (■) of ZnO microwells as functions of temperature in the range 81– 301 K.

3.3. Growth mechanism

Fig. 3 shows the morphologies of ZnO nanostructures on different areas along the downstream direction. As well known, interface structures determine the growth mechanisms, which include two kinds of growth mechanisms: smooth and rough interface growth mechanisms. Smooth interface growth is a layer-by-layer growth including 2D nucleus, dislocation and reentrant angle growth mechanism, following exponent growth rule. Rough interface growth is a continuous growth following a linear growth rule. When the furnace temperature suddenly is made to drop by turning off the power, Zn vapor pressure also drops but it is still above the over-saturation level. The driving force of 2D nucleation is lowered. So the {0 0 0 1} surface is not fully covered by the surface diffusion growth layer. With the driving force decreased, 1D linear growth is dominant accompanied with 2D growth. 1D NWs were grown on edges of the hexagonal cross-section surface [22]. It can be stated that NWs growth was along the step or screw dislocation curve. The 1D NWs growth is along the edge of steps in {0 0 0 1} smooth surface, shown in Fig. 3(a–f).

The growth mechanism includes 1D growth, 2D screw dislocation growth, and step growth or surface diffusion growth. When temperature drops further, the resultant different growth mechanism shows obviously different growth velocity because of the gradual weakening of the driving force. The 1D growth is the first, the screw dislocation the second and the surface diffusion the third. So the 1D structure is the preferred growth mechanism, as it is accompanied by screw dislocation and surface diffusion, roots of 1D structure emerge in surface diffusion, but the driving force is not large enough to make surface diffusion growth layer large enough to cover the full {0 0 0 1} surface and there is the circular hole left, as shown in Fig. 3, parts (g, h, i). The shape of ZnO NWs depends on the local temperature and on arriving ratio between zinc and oxygen atoms that arrive on the surface [23]. The local temperature has a prime effect on the degree of supersaturation. It illustrates that the degree of supersaturation determines the prevailing growth morphology. In a lower temperature region, zinc pressure drops swiftly and oxygen pressure increases relatively. The agglomeration of ZnO microwells was due to the rapid increase of oxygen pressure, [23] shown in Fig. 3(j).

3.4. Optical properties

The inset in Fig. 4 shows the intense green light emission at room temperature. Fig. 4 shows PL spectra at 81 K with a different excitation density. With increase in the excitation density, PL intensity of the UV-near-edge emission increases, while the PL intensity of the deep-level emission decreases. This abnormal phenomenon is attributed to surface and interface state effects of ZnO microwells. It suggests that the enhanced green emission is related to surface and interface state effects. To further elucidate it, the temperature dependence of PL spectra were measured, shown in Fig. 5(a). With temperature increase, the integrated PL intensity of the UV-near-edge emission decreases, while that of the deep-level emission increases at three different temperature intervals from 81 to 121 K, from 141 to 201 K and from 241 to 281 K, respectively, shown in Fig. 5(b). This abnormal phenomenon explains that the carriers trapped at surface state with a small active energy escaped from the bound state and contributed to the deep-level emission from 81 to 121 K. The abundant surface state and crystalline boundaries made the carriers get trapped at the defects with a different active energy. The trapped carriers with a large active energy gradually escaped when the temperature increases from 141 to 201 K and from 241 to 281 K, respectively. The integrated PL intensity of the deep-level emission also increased. The UV NBE emission intensity was not obviously increased with increase in temperature. So we infer that the excess carriers are excited by the green light. It is ascribed to the waveguide properties of ZnO microwells structures. The ultra-fine nanocrystals on the surface are with a different orientation. Therefore, the intense green light emission work as the light source to excite the ZnO NWs and the green light emission is enhanced.

4. Conclusion

The well-like ZnO nanostructures were obtained by chemical vapor deposition method. The microwells growth process was described as the cooperation of 1D linear growth mechanism and 2D diffusion mechanism. The abundant random range ultra-fine ZnO nanocrystals are on the surface of the ZnO nano-columns. The microwells have the waveguide properties. There is an abundance defects related to surface and interface states. The excess carriers trapped at surface state can escape with the temperature increase from 81 to 301 K and the green light emission was enhanced in the temperature-dependent PL spectra.

Acknowledgements

This work is supported by National High Technology Research and Development Program of China (2006AA03Z311), National Natural Science Foundation of China (Grant nos. 50725205, 60576040 and 60876014).

References

[1] Y.R. Lin, S.S. Yang, S.Y. Tsai, H.C. Hsu, S.T. Wu, I.-C. Chen, Cryst. Growth Des. 6 (2006) 1951.
[2] X.Y. Kong, Z.L. Wang, Nano Lett. 3 (2005) 1625.
[3] Z.W. Pan, S.M. Mahurin, S. Dai, D.H. Lowndes, Nano Lett. 5 (2005) 723.
[4] H. Zhang, D.R. Yang, D.S. Li, X.Y. Ma, S.Z. Li, D.L. Que, Cryst. Growth Des. 5 (2005) 547.
[5] U. Özgür, Y.I. Alivov, C. Liu, A. Teke, M.A. Reshchikov, S. Doğan, V. Avrutin, S.–J. Cho, H. Morkoc, J. Appl. Phys. 98 (2005) 041301.
[6] M.S. Arnold, P. Avouris, Z.W. Pan, Z.L. Wang, J. Phys. Chem. B 107 (2003) 659.
[7] Q.H. Li, Q. Wan, Y.J. Chen, T.H. Wang, H.B. Jia, D.P. Yu, Appl. Phys. Lett. 85 (2004) 636.
[8] Q. Wan, Q.H. Li, Y.J. Chen, T.H. Wang, X.L. He, J.P. Li, C.L. Lin, Appl. Phys. Lett. 84 (2004) 3654.
[9] L. Liao, H.B. Lu, M. Shuai, J.C. Li, Y.L. Liu, C. Liu, Z.X. Shen, T. Yu, Nanotechnology 19 (2008) 175501.
[10] X.D. Bai, P.X. Gao, Z.L. Wang, E.G. Wang, Appl. Phys. Lett. 82 (2003) 4806.
[11] X.H. Sun, S. Lam, T.K. Sham, F. Heigl, A. Jűrgensen, N.B. Wong, J. Phys. Chem. B 109 (2005) 3120.
[12] Z.L. Wang, X.Y. Kong, J.M. Zuo, Phys. Rev. Lett. 91 (2003) 185502.
[13] Z. Wang, X.F. Qian, J. Yin, Z.K. Zhu, Langmuir 20 (2004) 3441.
[14] B. Liu, H.C. Zeng, Langmuir 20 (2004) 4196.
[15] G.W. Sears, Acta Metall. 3 (1955) 367.
[16] Y.N. Xia, P.D. Yang, Y.G. Sun, Y.Y. Wu, B. Mayers, B. Gates, Y.D. Yin, F. Kim, H.Q. Yan, Adv. Mater. 15 (2003) 353.
[17] H.B. Huang, S.G. Yang, J.F. Gong, H.W. Liu, J.H. Duan, X.N. Zhao, R. Zhang, Y.L. Liu, Y.C. Liu, J. Phys. Chem. B 109 (2005) 20746.
[18] L. Vayssieres, Adv. Mater. 15 (2003) 464.
[19] D.X. Zhao, C. Andreazza, P. Andreazza, Chem. Phys. Lett. 399 (2004) 522.
[20] Y.H. Tong, Y.C. Liu, L. Dong, D.X. Zhao, J.Y. Zhang, Y.M. Lu, D.Z. Shen, X.W. Fan, J. Phys. Chem. B 110 (2006) 20263.
[21] S.H. Dalal, D.L. Baptista, K.B. Teo, R.G. Lacerda, Nanotechnology 17 (2006) 4811.
[22] X.D. Wang, J.H. Song, Z.L. Wang, Chem. Phys. Lett. 424 (2006) 86.
[23] L. Liao, J.C. Li, D.H. Liu, C. Liu, D.F. Wang, W.Z. Song, Q. Fu, Appl. Phys. Lett. 86 (2005) 083106.